Perovskite enhanced solid state ZnO solar cells

L Loh[1,2], J Briscoe[2] and S Dunn[2]
[1]School of Engineering, Nanyang Polytechnic, 180 Ang Mo Kio Ave 8, S568930, Singapore
[2]School of Engineering and Materials Science, Queen Mary, University of London, Mile End Road, London, E1 4NS, UK

E-mail: s.c.dunn@qmul.ac.uk

Abstract. This paper will report on the design, fabrication and testing of a solid-state perovskite enhanced ZnO solar cell. The p-type perovskite material used is bismuth ferrite (BFO) which has an absorption range within the blue range of the visible light spectrum. The solid state solar cell, was sensitized with N719 dye and used a CuSCN hole conductor. A disadvantage of ZnO is its poor chemical stability in acidic and corrosive environments. As chemical solution techniques were used in depositing BFO, a buffer method using an aminosilane ((3-aminopropyltrimethoxysilane or $H_2N(CH_2)_3Si(OCH_3)_3$)) coating was used to provide a protective coating on the ZnO nanorods before the BFO film was spin coated onto the ZnO nanorods. The photovoltaic performance of the solar cells were tested using a Keithley 2400 source meter under 100mW/cm^2, AM 1.5G simulated sunlight, where improvements in J_{sc} and efficiency were observed. The BFO was able to harness more electrons and also acted as a buffer from electron recombination.

Keywords: solar cell, perovskite, ZnO, BFO, CuSCN

INTRODUCTION

Since the development of the dye sensitised solar cell by Michael Gratzel[1,2], there has been a significant amount of research in solar cells using low cost materials and techniques. ZnO has been investigated as an alternative n-type material with its similar band structure and physical properties. ZnO has the advantage of higher electronic mobility and electron density (1 - 5 $cm^2V^{-1}S^{-1}$ and 1 – 5 x 10^{18} cm^{-3} respectively)[3] and has been studied using different nanostructures, doping of the semiconductor material, combining with composites, as well as using different processing technologies to improve the performance of the solar cell, which peaked at about 7%[4]. Liquid electrolytes used in redox systems, suffer from leakage, instability, dye desorption and corrosion of the electrodes[5]. Studies on solid-state solar cells where a solid hole conducting material is employed to replace the liquid redox electrolyte, have shown better stability. The use of the p-type semiconductor, copper thiocyanate (CuSCN) with a bandgap of 3.6 eV, hole conductivity of greater than 5×10^{-4} Scm^{-1}, chemical stability, transparency in the visible light spectrum range and high carrier mobility[6] has been reported with ZnO solar cells using various sensitizers. ZnO combined with sintered CdSe gave a stabilized efficiency of 1.5%. 0.1% efficiency was achieved using ZnO nanorods sensitized by *(cis-bis bis(2,2'-bipyridyl-4,4'-dicarboxylato) isothiocyanato ruthenium(II) bis-tetrabutylammonium) or* N719 dye for 1.8 μm length ZnO nanorods [7] and 1.7% efficiency[8] using 11-12 μm long ZnO nanorods.

The use of perovskite materials to display a PV effect was first investigated by Brady et al[9] in 1939 on tartaric acids. Since the 1970s, perovskite materials such as barium titanate ($BaTiO_3$)[10] and lead zirconate titanate (PZT)[11,12] have been studied for their ferroelectric properties which were

attributed to the non-centrosymmetry of the crystal structure. The use of perovskite-like materials like $CH_3NH_3PbI_3$[13–15] and $CsSnI_3$[16] recently received significant interest when they were shown to produce high performance TiO_2-based dye sensitized solar cells.

This paper will report the enhancements in performance on ZnO-based dye sensitized solid state solar cells using perovskite, Bismuth Ferrite ($BiFeO_3$ or BFO). The interest in BFO was initiated in 2003[17,18] where the photoconductivity was studied. BFO possesses an R3c space group, which exhibits weak ferromagnetism at room temperature, ferroelectric and piezoelectric properties below the Curie temperature of 1100 K and anti-ferromagnetic ordering below the Néel temperature of 640 K. BFO has been applied in solar cell applications in a few instances, and this includes a biotemplated synthesized BFO mesoporous-iodide electrolyte-based DSSC[19], in a CNT/BFO/Pt structure with CdSe quantum dots [20,21] as an electron conductor and in an inorganic-organic BFO/P3HT/Au hybrid solid state solar cell where BFO is classified by the authors as an n-type semiconductor to P3HT's p-type material[22].

EXPERIMENTS

2 mm thick glass with fluorine tin oxide (FTO) coating of 15Ω were used as substrates. A seed layer of ZnO was deposited using an aqueous method with 5mM of absolute ethanolic zinc acetate ($Zn(CH_3CO_2)_2$) by dropping on the conductive face of the substrate. The substrates were rinsed with ethanol and dried with nitrogen. The process was repeated 5 times before going through an annealing cycle on a hot plate at 350°C. The whole process was repeated 3 times. The growth of the ZnO nanorods were synthesized by an aqueous method. The seeded substrates were suspended face down in a fixture in 25mM of zinc nitrate hexahydrate ($Zn(NO_3)_2.6H_2O$) and 25mM of hexamethylenetetramine or HMT ($C_6H_{12}N_4$) in deionised (DI) water[23] at 90°C for 2.5 hours. This process was repeated with a change in precursor solution for 6 times for a total of 15 hours of growth. An aminosilane buffer layer was deposited on the ZnO nanorods using 3-aminopropyltriethoxysilane or $H_2N(CH_2)_3Si(OC_2H_5)_3$. The ZnO nanorods were soaked in an aqueous solution of 4% by volume 3-aminopropyltriethoxysilane in toluene at 60°C for 30 minutes. The samples were then rinsed with toluene and dried at 90°C for an hour. The BFO sol was formulated from bismuth nitrate pentahydrate ($Bi(NO_3)_3.5H_2O$) and iron nitrate nonahydrate ($Fe(NO_3)_3.9H_2O$) mixed in 2-methoxyethanol ($CH_3OCH_2CH_2OH$), with 20% and 0.2% by volume of the dehydrating agent acetic anhydride ($(CH_3CO)_2O$) and ethanolamine respectively. The BFO sol was then spin coated at 5000 rpm onto the aminosilane coated ZnO nanorods and preannealed at 350°C for 3 minutes on a hotplate. Samples were annealed at 600°C for 1 hour. The samples were next soaked in 0.5mM of N719 dye for 15 hours, rinsed with absolute ethanol and dried with nitrogen. Dupont's 25 µm thick Surlyn barrier film was then laid around the active area to act as a spacer. The sample was then spray coated with CuSCN at 90°C using 0.2 M CuSCN in dipropyl sulfide. Au counter electrodes were sputtered using a Denton Vacuum Explorer 14 thermal evaporator using a power of 125 W, base pressure of 4×10^{-2} mTorr and working pressure of 100 mTorr at ambient temperature in 100% Argon (Ar) atmosphere.

RESULTS AND DISCUSSIONS

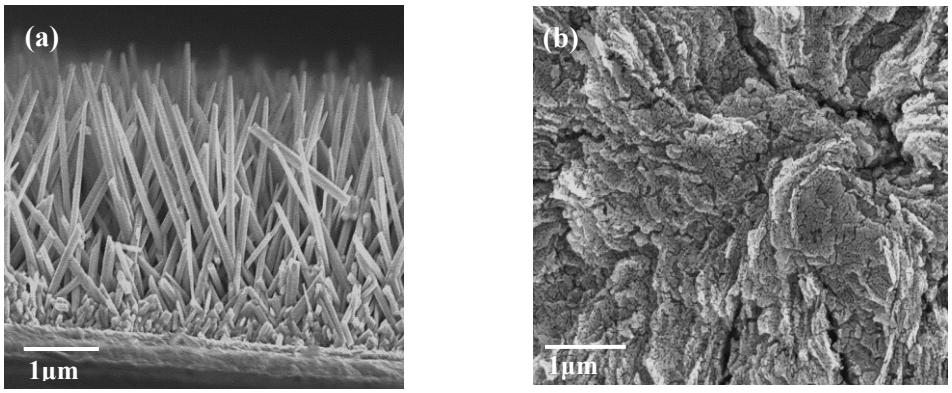

Figure 1. (a) Cross Sectional SEM Image of ZnO nanorods, (b) Dissolution of ZnO by BFO

The ZnO nanorods synthesized for 15 hours achieved about 2.3 µm long ZnO nanorods with (0001) crystallinity (Figure 1(a)). ZnO is chemically unstable in corrosive environments. The use of aminosilane buffer before the deposition of BFO was an important step as the BFO sol had a pH of less than 1. Direct deposition of BFO on the ZnO nanorods caused the dissolution of the ZnO nanorods(Figure 1(b)). The aminosilane was eventually removed during the annealing process of the ZnO/BFO nanorod structures. Figure 2 shows SEM images of the BFO coated ZnO nanorods. The TEM images show that the BFO had very thin coating which were particulate in nature, forming an almost hierarchical structure of nanorods coated with particles. Areas of even coating showed coatings of 1.4 nm – 2 nm thickness.

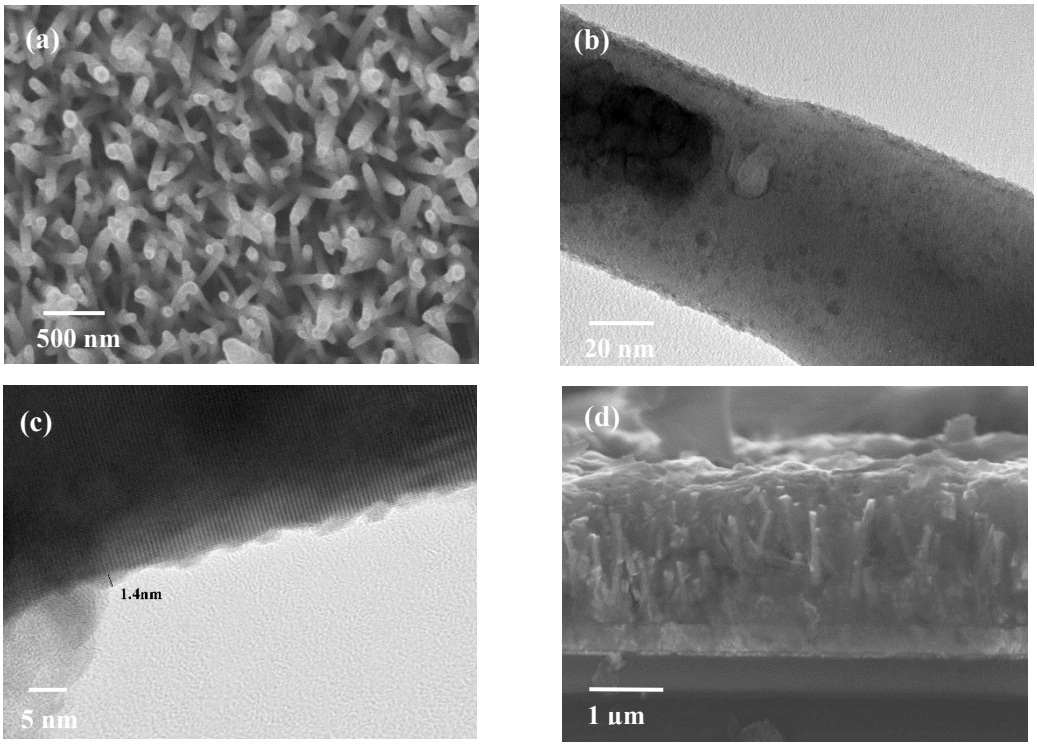

Figure 2. BFO coated ZnO nanorods: (a) SEM topographical view, (b) TEM image of evenly coated ZnO nanorod, (c) TEM image of 1.4nm thick BFO coating, (d) CuSCN infiltrated ZnO/BFO nanorods

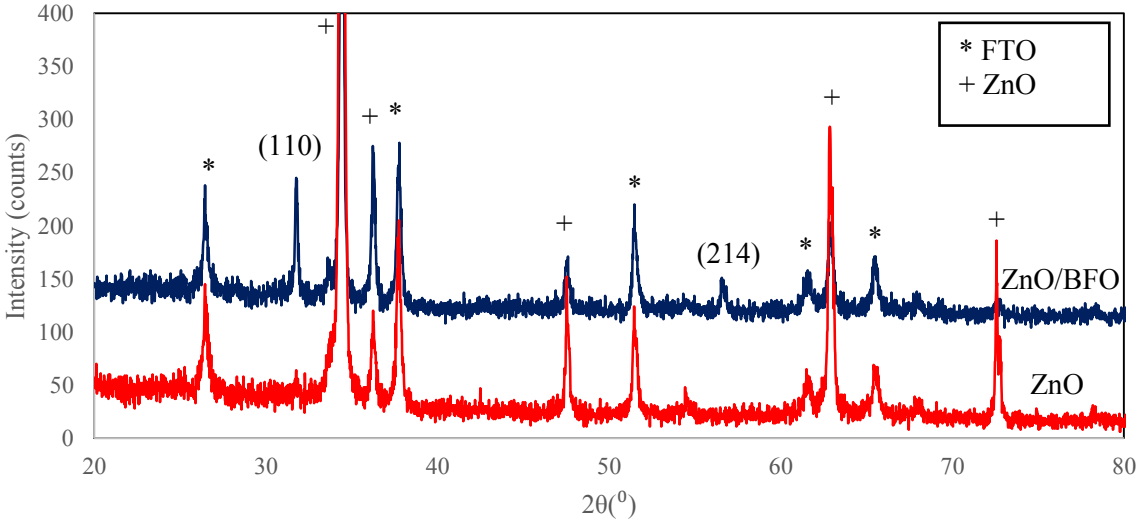

Figure 3. XRD comparison of ZnO nanorods and BFO coated ZnO nanorods

XRD scans of the samples in Figure 3, using the Panalytical X'pert Pro X-ray diffraction (XRD) confirm the presence of rhombohedral, R3c BFO crystallinity with a strong (110) crystal plane and a smaller (214) secondary BFO plane. The optical absorbance spectra in Figure 4, measured using the Perkin Elmer Lambda 950 UV visible spectroscopy showed the increased absorbance when BFO was added. There is a minor absorbance peak at around 517 nm indicating the presence of BFO.

The solar cells were tested with the IVT Solar VS 6820 solar simulator system with a Keithley 2400 source meter under 100mW/cm^2, AM 1.5G simulated sunlight. The J-V curves in Figure 5 showed a significant improvement in the performance of the solar cells with the addition of the BFO coating. There was a 100% increase in the J_{sc} and more than double the improvement in the efficiency.

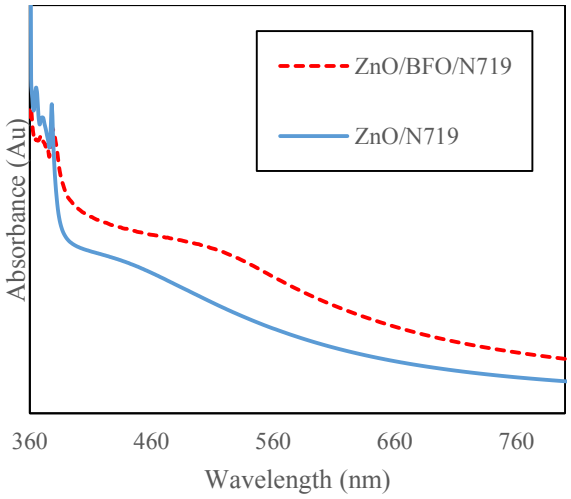

Figure 4. Comparison of absorbance data

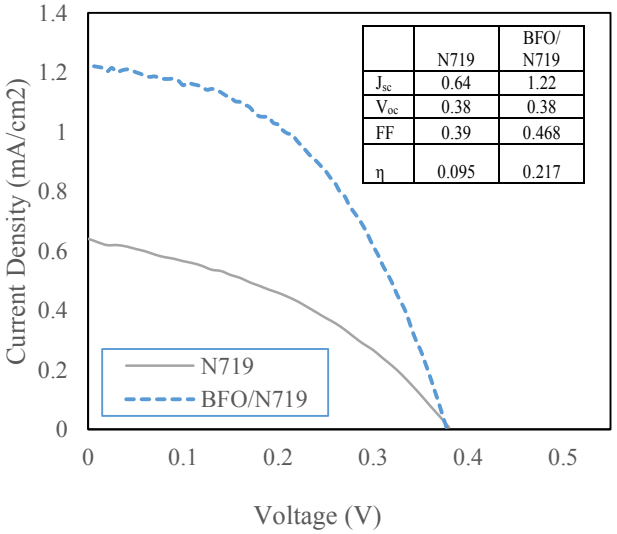

	N719	BFO/ N719
J_{sc}	0.64	1.22
V_{oc}	0.38	0.38
FF	0.39	0.468
η	0.095	0.217

Figure 5. Comparison of ZnO J-V curves

The indicative energy band diagram of the ZnO/BFO/N719/CuSCN is shown in Figure 6. The conduction band of N719 at 3.76 eV is lower than the 3.3 eV for BFO. On photoexcitation, the electrons tunnel through the BFO to the ZnO conduction band where the electrons are collected and flow through and external load to the counter electrode. The oxidised N719 and BFO via N719 is regenerated back to the ground state by capturing an electron from the valence band of the CuSCN via hole transfer. Recombination of the electrons occur with the N719 or with the CuSCN. However, with the lower N719 conduction band to the BFO's, the BFO acts as an electron blocking layer which helps suppress the electron recombination, thus resulting in the increased J_{sc} for the ZnO/BFO/N719 system.

CONCLUSION

In conclusion, we have shown that the addition of a BFO shell on ZnO nanorods was able to enhance the performance of a solid state solar cell with an increase in J_{sc} and having more than 2 times improvements in efficiency. BFO mainly acts as an electron blocker which prevents the electrons from recombining with the N719 due to the locations of their conduction bands. We have also shown that lower cost aqueous techniques can be used to deposit coatings using corrosive sols onto ZnO using a temporary buffer method. As a non-optimised construction of the solar cell was used, there is strong potential for improving the results further through optimised construction techniques.

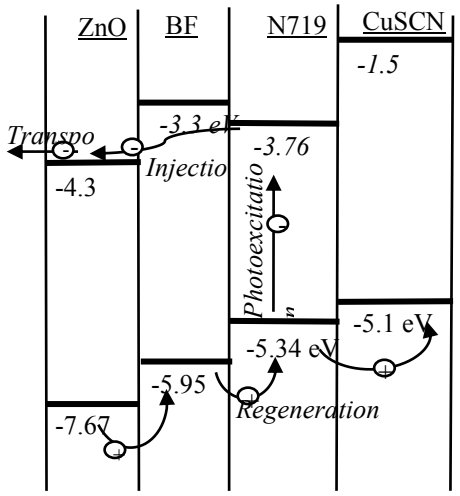

Figure 6. Representation of ZnO/BFO/ N719/CuSCN Energy

REFERENCES

1. Gratzel M 2005 *Inorg. Chem.* **44** 6841–51.
2. Gratzel M 2003 *J. Photochem. Photobio. C-Photochem.Rev*. **4** 145–53
3. Law M, Greene LE, Johnson JC, Saykally R and Yang PD 2005 *Nature Mat*. **4** 455–9
4. Xu CK, Wu JM, Desai U V and Gao D *J. Amer. Chem. Soc.* 2011 **133** 8122–5
5. Boschloo G and Hagfeldt A 2009 Accts. Chem. Res. **42** 1819–26
6. Zhang QB, Guo HH, Feng ZF, Lin LL, Zhou JZ and Lin ZH 2010 *Electrochimica Acta.* **55** 4889–94
7. Tena-Zaera R, Ryan MA, Katty A, Hodes G, Bastide S and Levy-Clement C 2006 *Comptes Rendus Chimie* **9** 717–29
8. Edri E, Rabinovich E, Niitsoo O, Cohen H, Bendikov T and Hodes G 2010 *J. Phys. Chem. C.* **114** 13092–7
9. Dittrich T, Kieven D, Rusu M, Belaidi A, Tornow J, Schwarzburg K, et al. 2008 *Appl. Phys. Lett.* **93**
10. Postels B, Kasprzak A, Buergel T, Bakin A, Schlenker E, Wehmann HH, et al 2008 *J. Kor. Phys. Soc.* **53** 115–8
11. Desai U V, Xu CK, Wu JM and Gao D 2012 *Nanotechnology* **23**
12. Etgar L, Gao P, Xue ZS, Peng Q, Chandiran AK, Liu B, et al. 2012 *J. Amer. Chem. Soc.* **134** 17396–9
13. Kim H-S, Lee J-W, Yantara N, Boix PP, Kulkarni SA, Mhaisalkar S, et al 2013 *Nano Lett.* **13** 2412–7
14. Kojima A, Teshima K, Shirai Y and Miyasaka T 2009 *J. Amer. Chem. Soc.* **131** 6050
15. Chung I, Lee B, He JQ, Chang RPH and Kanatzidis MG 2012 *Nature* **485** 486–494
16. Brody PS and Crowne F 1975 J. Elect. Mat. **4** 955–71
17. Glass AM, Linde DVD and Negran TJ 1974 *Appl. Phys. Lett.* **25** 233–5
18. Basu SR, Martin LW, Chu YH, Gajek M, Ramesh R, Rai RC, et al. 2008 *Appl. Phys. Lett.* **92** 91905
19. Nuraje N, Dang XN, Qi JF, Allen MA, Lei Y and Belcher AM. 2012 *Adv. Mat.* **24** 2885–9
20. Zang YY, Xie D, Chen Y, Wu X, Ren TL, Zhu HW, et al. 2012 *J. .Appl. Phys*. **112**
21. Zang YY, Xie D, Chen Y, Wu X, Ren TL, Wei JQ, et al. 2012 *Nanoscale* **4** 2926–30
22. Liu ZK and Yan F 2011 *Physica Status Solidi-Rapid Res. Lett.* **5** 367–9
23. Zhang QF, Dandeneau CS, Zhou XY and Cao GZ 2009 *Adv. Mat.* **21** 4087–108